

SUPPORTING INFORMATION

Mechano-induced reversible colour and luminescence switching of a gold(I)-diphosphine complex

Péter Baranyai,^a Gábor Marsi,^a Csaba Jobbágy,^a Attila Domján,^b Laura Oláh^a and Andrea Deák^{a*}

Hungarian Academy of Sciences, MTA TTK SZKI
^a”Lendület” Supramolecular Chemistry Research Group
^bNMR Research Group
1117 Budapest, Magyar Tudósok körútja 2., Hungary
E-mail: deak.andrea@ttk.mta.hu

General Procedures and Physical Measurements

All chemicals and solvents used for the syntheses were of reagent grade. The solvents for synthesis were used without further purification. All manipulations were performed in air.

Mechanochemical reaction was performed by a Retsch MM400 shaker mill in a 10 mL agate jar with two 10 mm diameter agate balls operating at 25 Hz. The elemental analysis has been carried out with an Elementar Vario EL III apparatus.

Solution-state NMR experiments were carried out on Varian Inova (400 MHz for ^1H) and Varian NMR SYSTEM (600 MHz for ^1H) spectrometers using a switchable broadband $X\{^1\text{H}\}$, and an inverse detection triple tuneable pfg 5mm $^1\text{H}^{13}\text{C}\{X\}$ probe ($X = ^{31}\text{P}$) respectively. Samples were placed into 5 mm NMR tube and the measuring temperature was 25 °C. ^1H chemical shifts are referenced to the residual solvent signal (CD_3OD : 3.31 ppm). ^{31}P shifts are given relative to the external reference 85% H_3PO_4 . Deuterated (99.98 atom%) solvent was purchased from Merck® GmbH, Germany. ^1H spectra were recorded with 16 seconds, while the ^{31}P spectra with 12 seconds relaxation delay and WALTZ-16 proton decoupling. The high resolution mass measurements were performed using a Q-TOF Premier mass spectrometer (Waters Corporation, 34 Maple St, Milford, MA, USA) in positive electrospray mode. Conductivity measurements were performed using three-electrode cell connected to a Radelkis OK-102/1 conductivity meter. The cell constant of the equipment was determined by calibration measurement using aqueous potassium chloride solution. The temperature was thermostated at 298 K. The measured specific conductivity was converted to molar conductivity, $\Lambda = \kappa/c$, where c is the solute concentration ($\text{mol} \cdot \text{L}^{-1}$). The UV-VIS spectra in solution and solid-phase were measured on an Agilent 8452A photodiode array spectrometer. The UV-VIS experiment used sample solution of 10 μM . The microcrystalline pellet method was used for the solid-state UV-Vis absorption measurements. The disc was prepared by mixing 100 mg very finely powdered KBr and 100 μg sample. The mixture was then pressed under vacuum at 7 tons with a standard KBr press for 3 min to provide a translucent disc. Diffuse reflectance UV-VIS spectra were recorded on an Edinburgh Instrument FLSP920 spectrofluorimeter using synchronous scan mode and the reflectance data were transformed by the Kubelka-Munk equation.¹ Finely powdered KBr was used as reflectance reference and samples were diluted by a factor of 10 with KBr. Steady state and time-resolved luminescence measurements were carried out on an Edinburgh Instrument FLSP920 spectrofluorimeter. Spectral corrections were applied using excitation and emission correction functions of the instrument. The solid-state room temperature emission studies were conducted on finely ground powder samples placed on a Quartz Suprasil plate in a front face sample holder. Low-temperature (77 K) emission measurements were recorded in glassy 2-methyltetrahydrofuran solution in a quartz capillary immersed in liquid nitrogen. Longpass filters were used to exclude the scattered excitation light. The excitation light source was a μF900H xenon flashlamp (pulse duration: 2 μs at FWHM) for the luminescent lifetime measurements. Powder diffractograms were produced with $\text{Cu-K}\alpha$ radiation on a vertical high-angle Philips PW 1050 powder diffractometer. Infrared spectra were recorded in the 400 to 4000 cm^{-1} spectral range on a Varian 2000 FT-IR spectrometer equipped with Golden Gate single reflection diamond ATR (Specac Ltd.). Optical micrographs were recorded with a LINKAM Imaging Station microscope equipped with Nikon DS-Fi1c digital camera. The thermogravimetric studies were performed using a simultaneous TG-DTA analyser (STA 6000, Perkin Elmer, Inc., Waltham, MA, USA), under nitrogen atmosphere (flow rate of 20 mL/min) in 0.07 mL open aluminium oxide pans. The sample mass was approximately 10 mg. The samples were heated from 30 °C to 280 °C at a constant heating rate of 10 °C/min.

Mechanochemical synthesis of Au(nixantphos)(SCN) (**1W**)

The starting $[\text{Au}_2(\text{nixantphos})_2](\text{NO}_3)_2$ complex was prepared according to a published procedure.² The methanol-assisted mechanochemical anion-exchange reaction was carried out by ball-milling $[\text{Au}_2(\text{nixantphos})_2](\text{NO}_3)_2$ (324.2 mg, 0.2 mmol) with NaSCN in a 1:3 molar ratio (50% excess) with addition of 80 μL methanol for 5 minutes. The mechanochemical reactions produce a powder mixture which after thorough washing with water provided pure anion-exchanged complex. Yield: 0.590 g (91%); FT-IR data: 3255 (m, br), 3188 (w), 3053 (m), 2989 (w), 2070 (s), 1568 (m), 1479 (w), 1454 (s), 1435 (s), 1404 (s), 1296 (m), 1270 (m), 1206 (m), 1183 (m), 1096 (m), 998 (w), 773 (m), 745 (m), 736 (m), 692 (m), 517 (w); Elemental analysis calcd. (%) C 55.09, H 3.37, N 3.47; found: C 54.82, H 3.49, N 3.19.

The limiting molar conductivity (Λ) obtained for complex **1W** is $103 \text{ S cm}^2 \text{ mol}^{-1}$ in methanol and $6 \text{ S cm}^2 \text{ mol}^{-1}$ in dichloromethane.

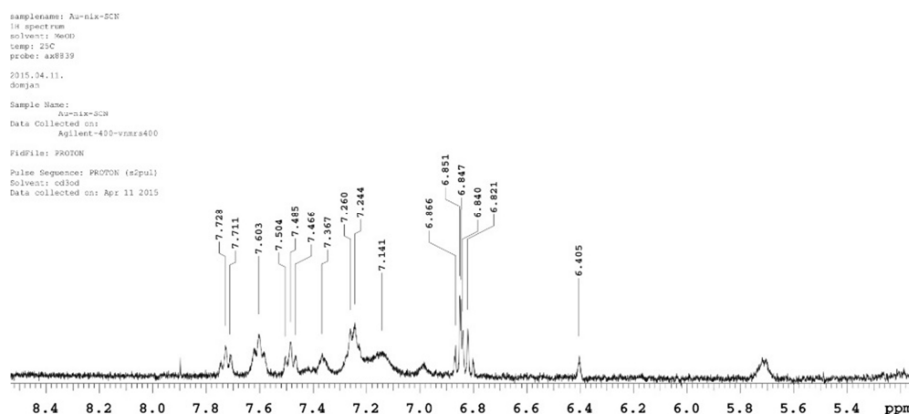


Fig. S1. ¹H NMR spectrum of **1W** recorded in CD₃OD.

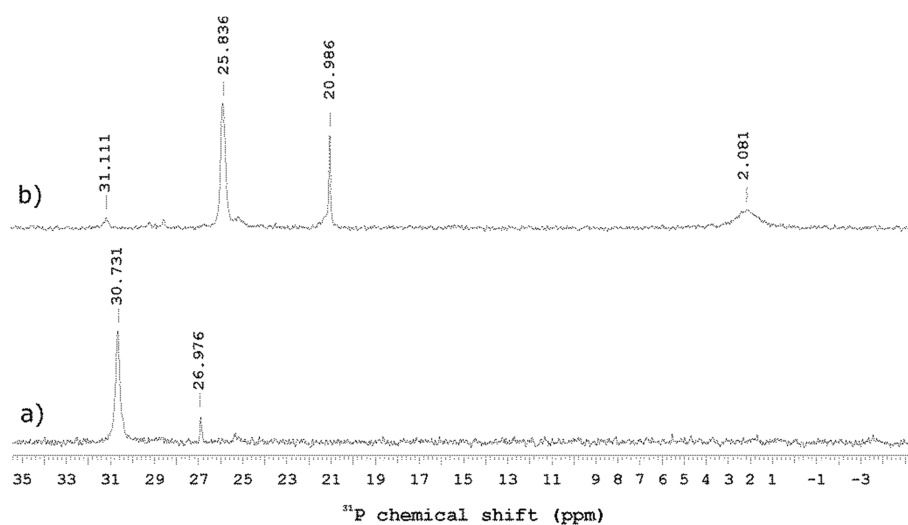


Fig. S2. ³¹P NMR spectra of **1W** recorded in a) CD₃OD and b) CD₂Cl₂.

ESI mass spectra recorded in the positive ion mode of **1W** in methanol and dichloromethane are depicted in Figure S3a and S3b, respectively. In the mass spectra of compound **1W** recorded in methanol, the predominant mass peak corresponds to the dimer $[\text{Au}_2(\text{nixantphos})_2]^{2+}$ cations (m/z 748.5 (100 %)), but mass peak corresponding to the monomer $[\text{Au}(\text{nixantphos})]^+$ cations (m/z 748.1 (76 %)) is also observed. In the mass spectra of **1W** recorded in dichloromethane, the predominant mass peak correspond to the monomer $[\text{Au}(\text{nixantphos})]^+$ cations (m/z 748.1 (100 %)), however dimer $[\text{Au}_2(\text{nixantphos})_2]^{2+}$ cations (m/z 748.5 (21 %)) are also present.

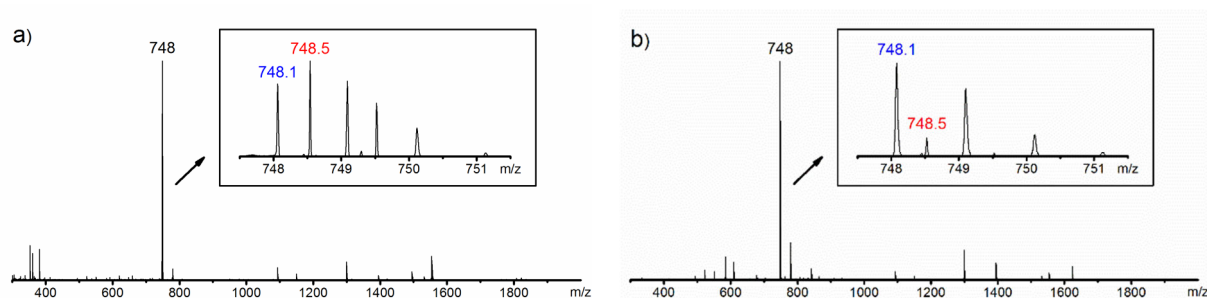


Fig. S3. ESI-MS spectra of **1W** recorded in a) methanol and b) dichloromethane.

X-ray Crystallography and Data Collection

Diffraction quality single crystals (Fig. S4) were obtained by slow evaporation of a methanolic solution of **1W**.

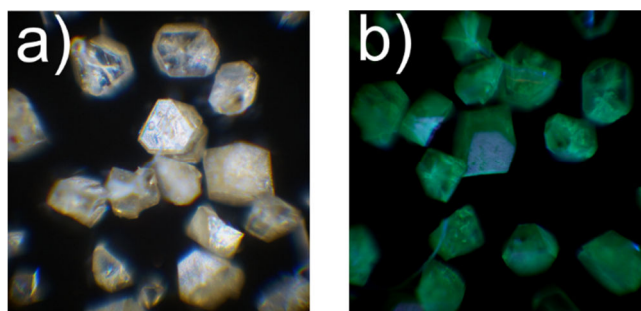


Fig. S4. Crystals of **1W** a) under ambient light and b) under 365 nm UV light.

Crystal of **1W** was mounted in Paratone-N oil within a conventional cryo-loop, and intensity data were collected on a Rigaku R-AXIS RAPID image plate diffractometer ($\lambda(\text{Mo-}K_{\alpha}) = 0.71070 \text{ \AA}$), fitted with an X-stream low temperature attachment (Table S1). Several scans in the φ and ω direction were made to increase the number of redundant reflections, which were averaged over the refinement cycles. All calculations were carried out using the *WinGX* package of crystallographic programs.³ The structures were solved by direct method (*SIR92*)⁴ and refined by full-matrix least-squares (*SHELXL-97*).⁵ All non-hydrogen atoms were refined anisotropically in F^2 mode. Hydrogen atomic positions were generated

from assumed geometries. The riding model was applied for the hydrogen atoms. Features of *WinGX*,³ *PLATON*⁶ and *Mercury*⁷ were used for data analysis. The structure was deposited at the Cambridge Data Centre and allocated with CCDC 1062108 number.

Table S1 Crystal data and structure refinement parameters for **1W**.

Formula	C ₃₇ H ₂₇ AuN ₂ OP ₂ S
Formula weight	806.57
Crystal size [mm]	0.23 × 0.28 × 0.39
Colour	colourless
Crystal system	triclinic
Space group	<i>P</i> -1
Temp. (K)	93
<i>a</i> [Å]	11.0432(5)
<i>b</i> [Å]	12.5167(6)
<i>c</i> [Å]	13.2977(5)
α [°]	93.219(2)
β [°]	113.830(3)
γ [°]	110.676(1)
<i>V</i> [Å ³]	1530.04(12)
<i>Z</i>	2
<i>d</i> _{calc} [Mg/m ³]	1.751
μ [mm ⁻¹]	5.015
No. of obsd. reflns. <i>I</i> > 2 σ (<i>I</i>)	8213
No. of parameters	400
GOOF	1.03
<i>R</i> 1 (obsd. data)	0.0327
<i>wR</i> 2 (all data)	0.0896

Grinding time-dependent mechanochromic and mechanochromic luminescence studies

1W was subjected to a mechanical stress in a Retsch MM400 shaker mill operating at 25 Hz. 600 mg crystalline sample of **1W** was placed into a 10 mL agate jar with two 10 mm diameter agate balls. At intervals of 1, 2, 3, 4, 5, 7, 10, 13, 18, 25 and 30 minutes of grinding time a small aliquot was extracted from the ball-milled sample for the photoluminescence, diffuse reflectance ultraviolet-visible spectroscopy, PXRD and FTIR measurements.

Grinding time-dependent FTIR spectra of **1W** are shown in Figure S5.

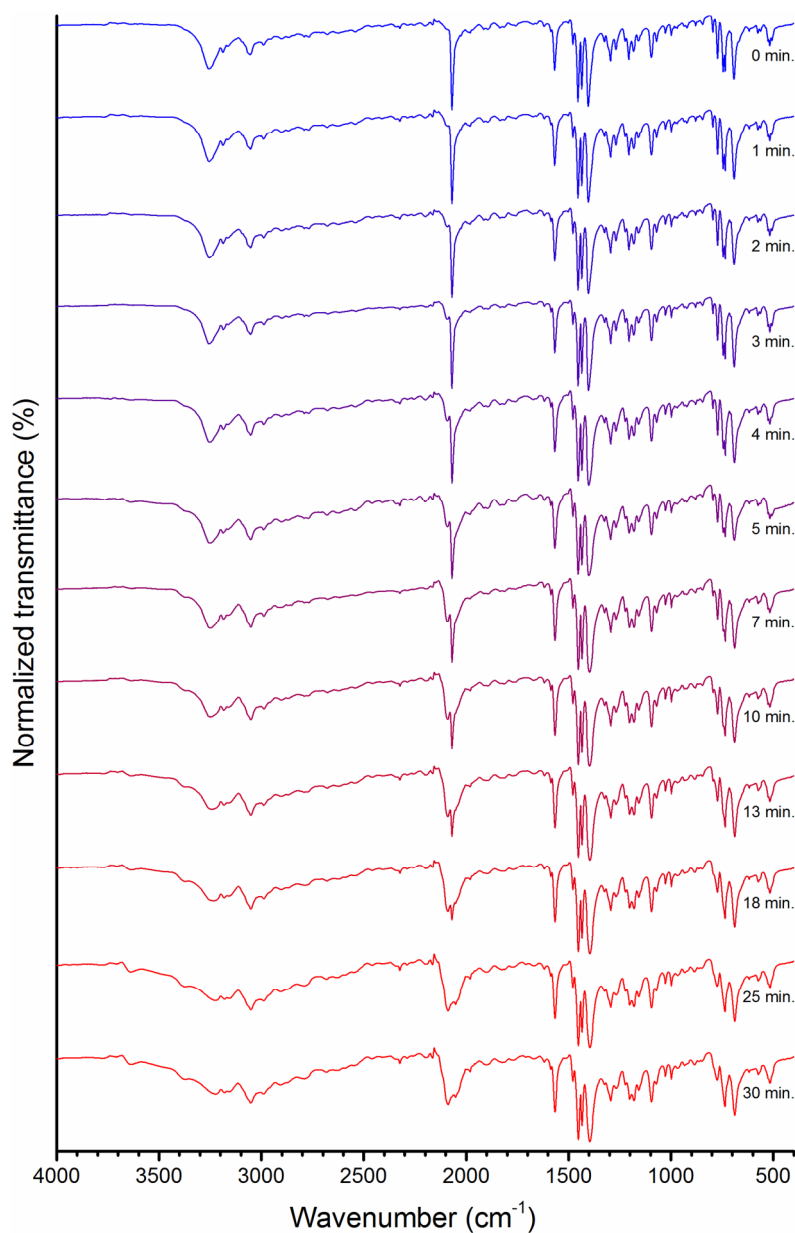


Fig. S5. Grinding time-dependent FTIR spectra recorded for **1W** before, and upon mechanical grinding.

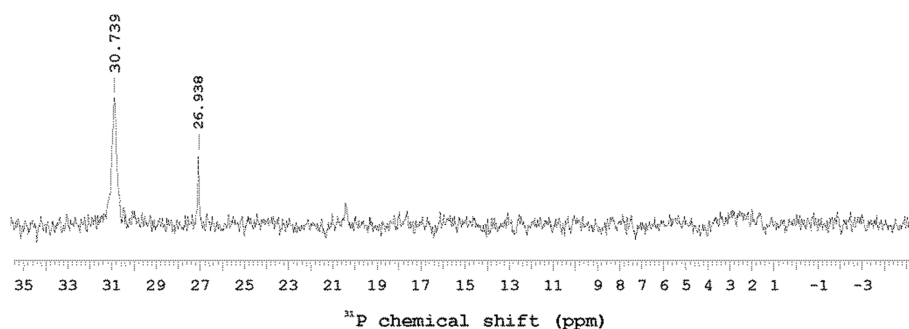


Fig. S6. ^{31}P NMR spectrum of **1Y** recorded in CD_3OD .

We also compared the positive ion mode ESI mass spectra of **1Y** in methanol (Fig. S7a) and dichloromethane (Fig. S7b). In both cases, the mass spectra show the presence of dimer $[\text{Au}_2(\text{nixantphos})_2]^{2+}$ cations (m/z 748.5) and monomer $[\text{Au}(\text{nixantphos})]^+$ cations (m/z 748.1) differing from each other in terms of relative intensities. In the ESI mass spectrum of compound **1Y** recorded in methanol, the predominant mass peak corresponds to the dimer $[\text{Au}_2(\text{nixantphos})_2]^{2+}$ cations (m/z 748.5 (100 %)), while the ESI MS spectrum of the same **1Y** sample recorded in dichloromethane shows a predominant mass peak at m/z 748.1 corresponding to the monomer $[\text{Au}(\text{nixantphos})]^+$ cations (100 %).

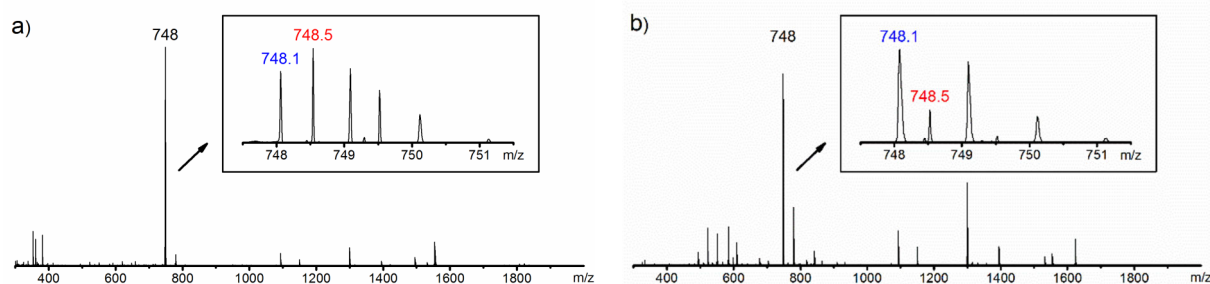


Fig. S7. ESI-MS spectra of **1Y** recorded a) in methanol and b) dichloromethane.

Luminescence spectroscopic studies of **1W** and **1Y**

Additional spectroscopic investigations were performed to reveal the photophysics of **1W** and **1Y** forms. The dichloromethane and 2-methyltetrahydrofuran solutions of **1W** are non-luminescent upon UV excitation at room temperature, but intense blue emission is perceived in degassed 2-methyltetrahydrofuran glass at 77 K (Fig S8a). The luminescence lifetimes are 2.8 and 980 ms for **1W** and nixantphos ligand, respectively. Resemblance among the emission spectra of the neutral **1W** at room temperature and glassy 2-methyltetrahydrofuran solutions of **1W** and nixantphos ligand at 77 K indicates that the luminescence of solid **1W** originates from an intraligand type excited state. The amorphous phase **1Y** and reported dinuclear **1N** complex show very similar, structureless emission bands (Fig S8b) having short lifetimes (0.3 μ s for **1N**),⁸ which suggests that the intramolecular aurophilic interaction may be responsible for the broad and red-shifted luminescence.

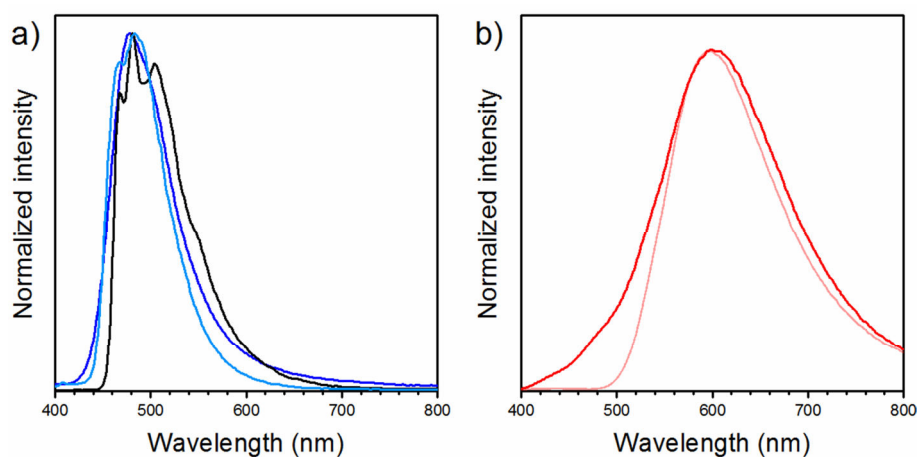


Fig. S8. a) Emission spectra of **1W** (blue line) at 298 K, **1W** (light blue line) and nixantphos ligand (black line) in glassy 2-methyltetrahydrofuran at 77 K b) emission spectra of **1Y** (red line) and **1N** (light red line).

General procedure for reversible crystalline-to-amorphous (CTA) and amorphous-to-crystalline (ATC) transformations

250 mg of **1W** was ball-milled for 15 minutes, resulting in completely amorphous **1Y**. After methanol treatment, the amorphous **1Y** converted back into crystalline **1W**. Thus, the original white colour and blue luminescence restored when the yellow-coloured red emitting **1Y** was exposed to methanol vapour. The newly form **1W** shows an emission spectrum identical to that of pristine **1W** (Fig. S9a) and sharp diffraction peaks emerge again (Fig. S9b).

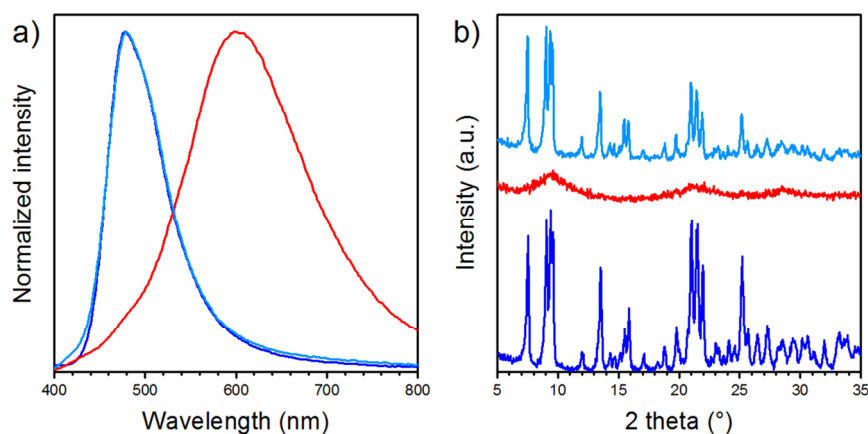


Fig. S9. a) Emission spectra and b) PXRD patterns of **1W** (blue line), amorphous **1Y** obtained from CTA transformation (red line) and **1W** obtained from ATC transformation (light blue line).

The dynamic switching process between blue and red luminescence can be repeated many times by using subsequent grinding and solvent fuming cycles. The emission characteristics and lifetimes of crystalline **1W** and amorphous **1Y** obtained in four subsequent grinding and solvent fuming cycles are listed in Table S2. The different synthesis routes and/or crystalline size may be responsible for faster decays observed in case of samples of **1W** obtained from CTA transformations compared to the pristine **1W** obtained by mechanochemical synthesis.

Table S2. Emission characteristics and lifetimes of crystalline **1W** and those of **1W** obtained from ATC transformation, as well as their corresponding amorphous **1Y** forms obtained from CTA transformation.

Compound	Cycle No.	λ_{em} (nm)	τ_1 (μ s)	τ_2 (μ s)
1W	–	478	11 (27%)	39 (73%)
1W from ATC	1	479	3.4 (57%)	15 (43%)
	2	479	4.5 (63%)	20 (37%)
	3	479	5.6 (65%)	27 (35%)
	4	479	2.8 (71%)	21 (29%)
1Y from CTA	1	603	0.6 (74%)	4.3 (26%)
	2	606	0.5 (81%)	3.3 (19%)
	3	611	0.7 (81%)	4.0 (19%)
	4	606	0.5 (79%)	3.8 (21%)

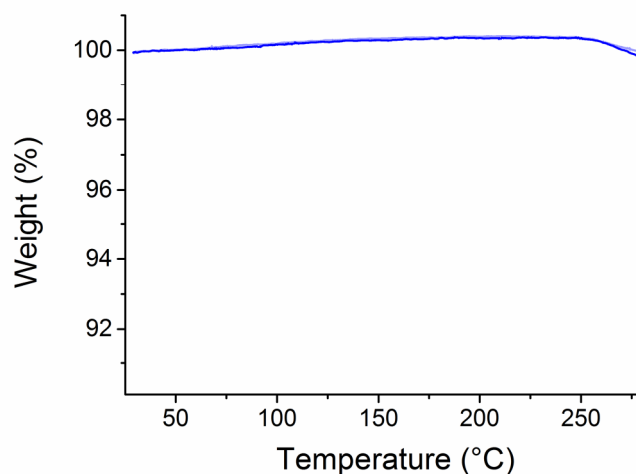


Fig. S10. TG analysis of pristine **1W** (blue line) and **1W** obtained from ATC transformation (light blue line).

Acknowledgement

The authors gratefully acknowledge the support by MTA (Hungarian Academy of Sciences) through the Lendület Programme (LP2012-21/2012). We thank Dr. Alfréd Kállay-Menyhárd (Laboratory of Plastics and Rubber Technology, Department of Physical Chemistry and Materials Science, Budapest University of Technology and Economics, Budapest, Hungary) for TGA measurements and Dr. Ágnes Gömöröy (Instrumentation Center, Research Centre for Natural Sciences, Hungarian Academy of Sciences, Budapest, Hungary) for recording the ESI mass spectra.

References

1. a) P. Kubelka, F. Munk, *Z. Technol. Phys.* 1931, **12**, 593; b) P. Kubelka, *J. Opt. Soc. Am.* 1947, **38**, 448.
2. T. Tunyogi, A. Deák, G. Tárkányi, P. Király, G. Pálincás, *Inorg. Chem.* 2008, **47**, 2049.
3. L. J. Farrugia, *J. Appl. Cryst.* 2012, **45**, 849.
4. A. Altomare, G. Cascarano, C. Giacovazzo, A. Guagliardi, M. C. Burla, G. Polidori, M. J. Camalli, *Appl. Cryst.* 1994, **27**, 435.
5. G. M. Sheldrick, *SHELXL, Version 2014/7*, Program for Crystal Structure Refinement, University of Göttingen, 2014.
6. A. L. Spek, *Acta Cryst.* 2009, **D65**, 148.
7. C. F. Macrae, P. R. Edgington, P. McCabe, E. Pidcock, G. P. Shields, R. Taylor, M. Towler, J. van de Streek, *J. Appl. Cryst.* 2006, **39**, 453.
8. A. Deák, Cs. Jobbágy, G. Marsi, M. Molnár, Z. Szakács, P. Baranyai, *Chem. Eur. J.* 2015, **21**, in press.